

# Ferromagnetic insulating state in manganites: $^{55}\text{Mn}$ NMR study

M. M. Savosta, V. I. Kamenev, V. A. Borodin

*Donetsk Institute of Physics & Technics, Academy of Sciences of Ukraine, Rozy Luxembourg 72, 83114 Donetsk, Ukraine*

P. Novák, M. Maryško, J. Hejtmánek

*Institute of Physics, Academy of Sciences of the Czech Republic, Na Slovance 2, 182 21 Praha 8, Czech Republic*

K. Dörr, M. Sahana

*Institute of Solid State and Materials Research, IFW Dresden, P.O.B. 270016, D-01171 Dresden, Germany*

A. Shames

*Department of Physics, Ben-Gurion University of the Negev, P.O. Box 653, 84105, Be'er-Sheva, Israel*

(March 22, 2022)

$^{55}\text{Mn}$  NMR was used to study the ferromagnetic insulating state in four different manganites. In all cases the coexistence of two types of regions possessing different NMR spectra and nuclear spin dynamics was found. In the ferromagnetic insulating clusters the hopping frequency  $f_{hop}$  of the electron holes is slower comparing to the NMR frequency  $f_{res}$  and two lines ascribed to  $3+$  and  $4+$  valence state of Mn are observed. The relaxation rate increases rapidly with the increasing temperature, so that these spectra can no longer be detected for temperatures higher than  $\approx 60$  K. In ferromagnetic metallic clusters  $f_{res} < f_{hop}$  and the motionally narrowed spectrum is observed in a broad temperature interval, as the relaxation remains only moderately fast.

## I. INTRODUCTION

Hole-doped manganites  $\text{La}_{1-x}\text{A}_x\text{MnO}_3$  ( $\text{A}=\text{Ca}, \text{Sr}, \text{Ba}, \text{Pb}$ ) have attracted much attention in recent years. The reason is not only the 'colossal' magnetoresistance that occurs in these systems, but also a rich variety of the physical phenomena including intrinsically inhomogeneous ground states, phase separation, charge/orbital ordering etc. [1]. The basic mechanism that couples the spin and charge in these materials and produces the ferromagnetic metallic-like (FMM) state is generally assumed to be described by the double exchange (DE) model. In this model, an electron hole tends to hop more easily between the two successive Mn sites if both Mn site moments are aligned. Rather intriguing is the existence of ferromagnetic but insulating (FMI) state, which is beyond the DE concept. FMI state may be realized in several ways, in particular it occurs when the doping is low, in the systems with strong disorder or distortions in the lattice or for certain substitutions on the Mn sites. The microscopic nature of these FMI states is far from being clear - several models, including charge and/or orbital ordering, superexchange ferromagnetic interactions, cluster-glass state, phase segregation between fer-

romagnetic metallic and insulating charge-ordered clusters, have been examined in this context [2–6].

NMR is a suitable tool to provide further insight in the nature of the FMI state as it probes locally the magnetic states and their dynamics. Ultraslow diffusion of the small Jahn-Teller (JT) polarons in several insulating  $\text{LaMnO}_{3+\delta}$  and  $\text{La}_{1-y}\text{Ca}_y\text{MnO}_{3+\delta}$  manganites, gives rise to an inhomogeneous loss and final disappearance of the  $^{139}\text{La}$  NMR signal when the temperature increases, as reported recently by Allodi *et al.* [7]. This 'wipeout' of the  $^{139}\text{La}$  NMR signal intensity in the FMI  $\text{La}_{1-x}\text{Ca}_x\text{MnO}_3$  was observed also by Papavassiliou *et al.* [8] and it was associated with a low frequency dynamics of the Mn octant cells. The  $^{55}\text{Mn}$  NMR in the corresponding systems was studied in several papers [9–12], the dynamics of the  $^{55}\text{Mn}$  nuclear spins, which is definitely an important item, was not addressed until now, however.

In this paper we present the results of detailed studies of the NMR spectra and relaxation on the  $^{55}\text{Mn}$  nuclei, completed in some cases by  $^{139}\text{La}$  NMR, for several FMI manganites, including two different self-doped  $\text{La}_{1-x}\text{Mn}_{1-y}\text{O}_3$ , low-doped  $\text{La}_{0.84}\text{Sr}_{0.16}\text{MnO}_3$ , and Ti-substituted  $\text{La}_{0.6}\text{Pb}_{0.4}\text{Mn}_{0.9}\text{Ti}_{0.1}\text{O}_3$  compounds. Two types of regions associated with the FMM and FMI clusters, possessing quite different nuclear spin dynamics and  $^{55}\text{Mn}$  NMR spectra, are detected for all compounds studied. The NMR spectra arising from the FMM clusters consist of a single motionally narrowed line, which is detected in a relatively broad temperature interval. The exception is  $\text{La}_{0.84}\text{Sr}_{0.16}\text{MnO}_3$  where more motionally narrowed lines are observed below the metal-insulator transition. The spin fluctuations on  $^{55}\text{Mn}$  nuclei in FMI clusters are in a slow fluctuation limit, i.e.  $f_{hop} < f_{res}$ . Corresponding spectra consist of two lines ascribed to  $\text{Mn}^{4+}$  and  $\text{Mn}^{3+}$  ions, and they can be detected for all compounds studied only for  $T < 60$  K. This behavior is in line with the recovery of the signal amplitude on the  $^{139}\text{La}$  nuclei in the same temperature interval. Two scenarios of the FMM to FMI transition depending on the different ratio of FMM and FMI clusters as well as possible nature of these clusters are discussed.

## II. EXPERIMENTAL

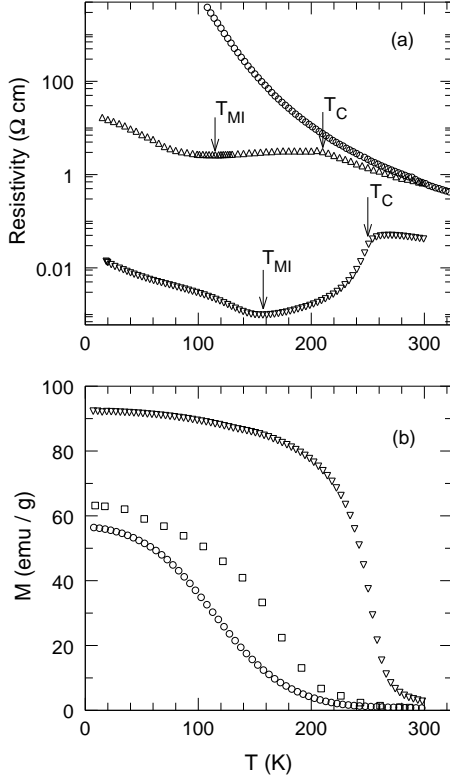


FIG. 1. Temperature dependence of the resistivity (a) and magnetization in an applied field of 0.5 T (b) for  $\text{La}_{1-\delta}\text{MnO}_3$  ( $\circ$ ),  $\text{La}_{0.94}\text{Mn}_{0.98}\text{O}_3$  ( $\triangle$ ), and  $\text{La}_{0.84}\text{Sr}_{0.16}\text{MnO}_3$  ( $\nabla$ ). Magnetization as a function of temperature for  $\text{La}_{0.6}\text{Pb}_{0.4}\text{Mn}_{0.9}\text{Ti}_{0.1}\text{O}_3$  measured in 0.3 T (lower panel,  $\square$ ).

The single crystal of  $\text{La}_{0.94}\text{Mn}_{0.98}\text{O}_3$  and polycrystalline compound  $\text{La}_{0.6}\text{Pb}_{0.4}\text{Mn}_{0.9}\text{Ti}_{0.1}\text{O}_3$  used in the present study were described in Refs. [13,14]. The single crystal  $\text{La}_{0.84}\text{Sr}_{0.16}\text{MnO}_3$  was grown by the floating zone method. The self-doped polycrystalline  $\text{La}_{1-\delta}\text{MnO}_3$  ( $\delta \approx 0.05$ ) was prepared by standard solid state reaction at 1000-1100°C for 50 hours with intermediate grinding and pressing. The temperature dependence of the electrical resistivity, measured with the standard four-probe method, and magnetization curves are shown in Figs. 1a,b. The resistivity of  $\text{La}_{0.84}\text{Sr}_{0.16}\text{MnO}_3$  exhibits a metallic-like behavior below  $T_C = 250$  K. As temperature decreases further, the curve shows an upturn in the ferromagnetic phase below the metal-insulator transition temperature  $T_{MI} = 157$  K. The FMI state ( $d\rho/dT < 0$ ) is realized below  $T_{MI}$ . A similar behavior is observed for  $\text{La}_{0.94}\text{Mn}_{0.98}\text{O}_3$  with  $T_C = 210$  K [13] and  $T_{MI} = 115$  K, though the value of the resistivity is by one to three orders of magnitude higher than that of  $\text{La}_{0.84}\text{Sr}_{0.16}\text{MnO}_3$ . The self-doped  $\text{La}_{1-\delta}\text{MnO}_3$  is an insulator, the onset of the magnetic ordering is at about 190 K. The resistivity of  $\text{La}_{0.6}\text{Pb}_{0.4}\text{Mn}_{0.9}\text{Ti}_{0.1}\text{O}_3$  ( $T_C = 180$  K) was not measured, but it is known that such level of Ti dop-

ing on the Mn site leads to an insulating behavior for  $\text{La}_{0.7}\text{Ca}_{0.3}\text{Mn}_{1-x}\text{Ti}_x\text{O}_3$  [15,16].

The NMR spectra were recorded by a two-pulse spin-echo method at temperatures between 22 and 250 K using a noncoherent home-build spectrometer with frequency sweep and boxcar detector signal averaging. The NMR spectra were obtained by measuring the integrated intensity of the spin-echo versus frequency using  $\tau = 3-4 \mu\text{s}$ , where  $\tau$  is the time separation between the two pulses. The spin-spin relaxation was studied by measuring the form of the spin-echo decay as a function of  $\tau$ . All the signals detected come from the regions with strong ferromagnetic correlations as follows from the characteristic high values of the enhancement factor  $\eta \approx 500-2500$ . The spin-echo amplitudes were corrected for the  $f^2$ -type frequency response and the  $1/T$  reduction, that results from the Curie law for the nuclear magnetic moment.

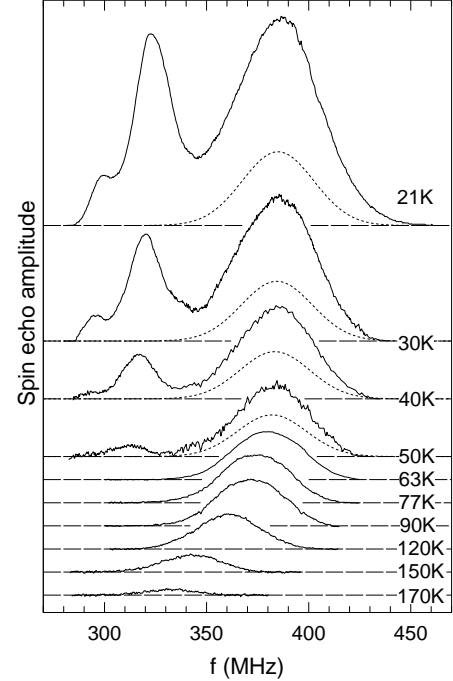


FIG. 2.  $\text{La}_{1-\delta}\text{MnO}_3$ .  $^{55}\text{Mn}$  NMR spectra taken at ten different temperatures. The dotted curves correspond to the contribution of the FMM clusters to the spectra.

## III. RESULTS AND DISCUSSION

The evolution of the  $^{55}\text{Mn}$  NMR spectra in  $\text{La}_{1-\delta}\text{MnO}_3$  with the temperature is displayed in Fig. 2. For  $T \geq 63$  K the NMR spectra consist of a single line similarly as found in conventional FMM manganites [17]. This line is attributed to a motional narrowing - the electron holes hop over the manganese sites with a rate faster than the frequency splitting  $\Delta f$  of the  $\text{Mn}^{3+}$  and  $\text{Mn}^{4+}$  resonances, and as a result all  $^{55}\text{Mn}$  nuclei feel the same averaged hyperfine field. The reduction of the spin-echo amplitude of this line with increasing  $T$  is

mainly connected with the shortening of the spin-spin relaxation time  $T_2$ , which becomes comparable to the time separation  $\tau$ . Below 63 K the NMR spectrum qualitatively changes, as new contributions gradually develop. The line at around 320 MHz corresponds to the  $\text{Mn}^{4+}$  resonance [17]. The satellite line at around 300 MHz, which may be attributed to a  $\text{Mn}^{4+}$  resonance for specific Mn sites, is observed only in this sample and it will be discussed later. More important, the amplitude of the signal at about 390 MHz increases substantially below 63 K, indicating additional contribution in this frequency region too.

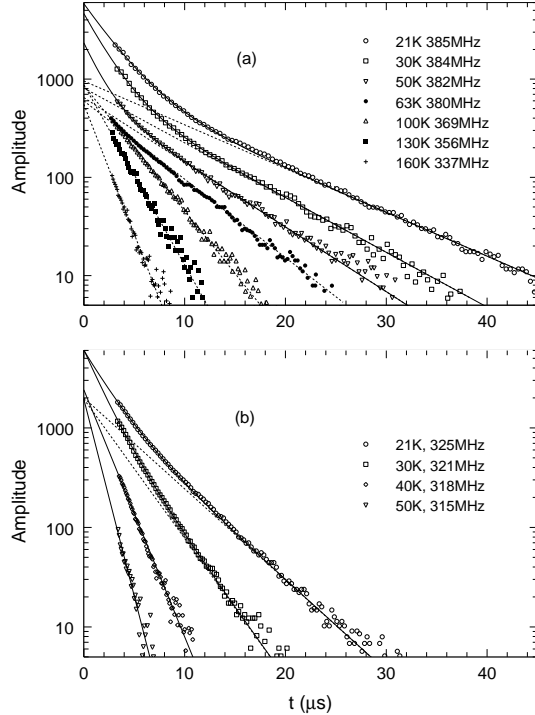


FIG. 3.  $\text{La}_{1-\delta}\text{MnO}_3$ . Spin-echo decay at the maximum of the FMM line (a) and  $\text{Mn}^{4+}$  line (b). The solid curves correspond to the two-exponential fit, the dotted curves correspond to the slower relaxing component.

The spin-echo decays taken at the maximum of the motionally narrowed FMM line for different temperatures reveal this contribution (Fig. 3a). For  $T \geq 63$  K the decays are exponential,  $A = A_0 \exp(-2\tau/T_2)$ . The slope of the decays changes monotonically in the whole temperature range (taking the tail ends of the spin-echo decay curves for low  $T$ ), reflecting the temperature dependence of  $T_2$  for the FMM line. Moreover, the amplitude  $A_0$  of the FMM line, extrapolated to  $\tau=0$  (dashed lines in Fig. 3) is nearly constant in the limits of the experimental error  $\pm 20\%$ . The contribution of FMM line to the spectra at low temperatures is schematically shown in Fig. 2 by dotted curves. From the data in Fig. 3a it is clearly seen that the increase of the signal intensity below 63 K is due to an additional, fast relaxing contribution to the spin-echo decays. The possibility that this contribution

originates from the domain walls can be safely ruled out as it follows from the form of the spin-echo decays taken at different values of radiofrequency (rf) power (Fig. 4a). It is seen that the optimal value of the rf field for the fast relaxing component is four times larger compared to the one for FMM line. Thus, faster relaxing regions possess smaller NMR enhancement contrary to expected behavior of the NMR signal from the domain walls. The spin-spin relaxation of  $\text{Mn}^{4+}$  line is strongly temperature dependent, corresponding spin-echo decay curves are not of a single-exponential type (Fig. 3b). The form of the spin-echo decay is rather insensitive to the change of the rf field around its optimal value in this case (Fig. 4b), indicating certain distribution of relaxation times in the regions with the similar magnetocrystalline anisotropy.

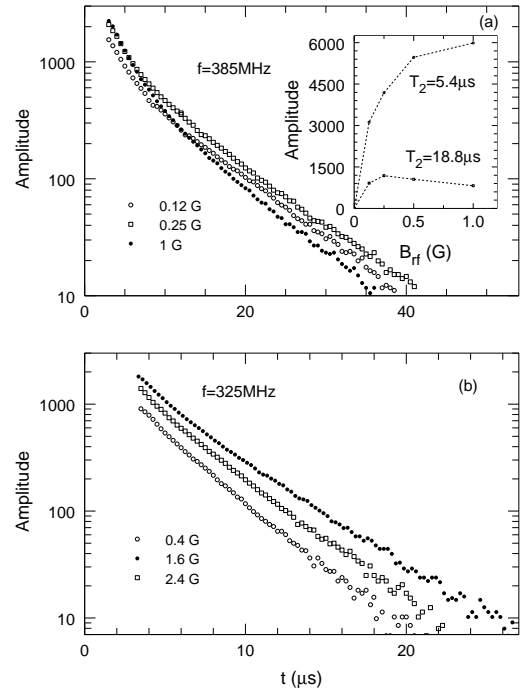


FIG. 4.  $\text{La}_{1-\delta}\text{MnO}_3$ . (a) Spin-echo decay at the maximum of the FMM line for three values of the rf power. In the inset the dependence of the spin-echo amplitude on the rf power is shown for slower relaxing component ( $T_2=18.8 \mu\text{s}$ ) and faster relaxing component ( $T_2=5.4 \mu\text{s}$ ) of the line. (b) Spin-echo decay at the maximum of the  $\text{Mn}^{4+}$  line for three values of the rf field around its optimal value.

The  $^{55}\text{Mn}$  NMR suggests that in  $\text{La}_{1-\delta}\text{MnO}_3$  two different types of ferromagnetic regions exist. In what follows these regions are called FMM and FMI clusters. The signal arising from the FMM clusters consists of a single motionally narrowed line, which is detected in relatively broad temperature interval thanks to the fact that corresponding spin-spin relaxation is only moderately fast. The FMI clusters give rise to two lines at about 320 and 390 MHz which can be detected only for  $T \leq 60$  K because of the inhomogeneous and very strongly temperature dependent spin-spin relaxation. As we show below

this picture is typical for all compounds studied. It is clear from Fig. 3 that the spin-spin relaxation strongly influences the amplitude of the NMR spectra even if the shortest  $\tau$  is used. To make the NMR spectra of remaining three compounds more representative, we tried to correct the line's amplitude for the measured spin-spin relaxation. The fits of corresponding spin-echo decays by two or single exponential were employed. We checked that a stretched exponential form of the fitting function, often used in the literature, would not affect our estimate of the temperature dependence of  $A_0$ .

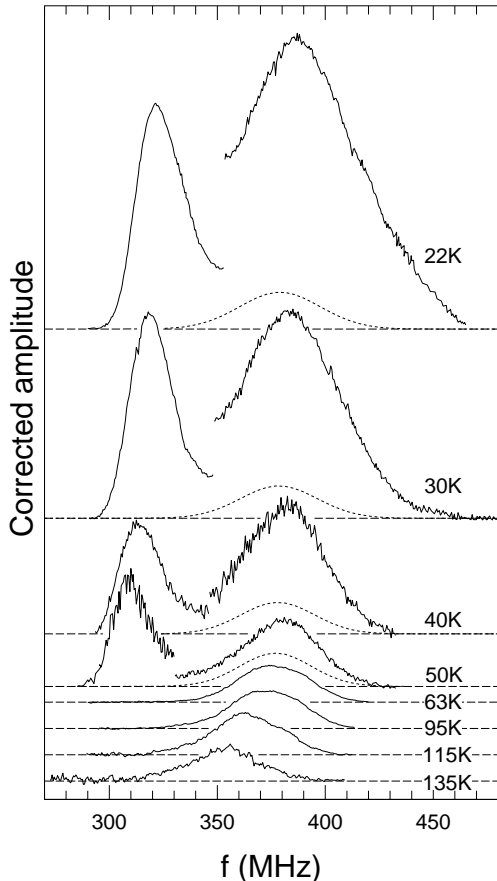


FIG. 5.  $\text{La}_{0.6}\text{Pb}_{0.4}\text{Mn}_{0.9}\text{Ti}_{0.1}\text{O}_3$ . Corrected  $^{55}\text{Mn}$  NMR spectra at several temperatures. The dotted curves correspond to the contribution of the FMM clusters to the spectra.

Corrected NMR spectra of  $\text{La}_{0.6}\text{Pb}_{0.4}\text{Mn}_{0.9}\text{Ti}_{0.1}\text{O}_3$ ,  $\text{La}_{0.94}\text{Mn}_{0.98}\text{O}_3$ , and  $\text{La}_{0.84}\text{Sr}_{0.16}\text{MnO}_3$  are presented in Figs. 5, 7, 8, respectively. The correction is qualitative only as for low and high frequency peaks we used the decay of the spin-echo signal at the corresponding amplitude maxima and neglected the fact that it changes continuously with the frequency. As a result a discontinuity appears in the corrected spectra. For  $\text{La}_{0.6}\text{Pb}_{0.4}\text{Mn}_{0.9}\text{Ti}_{0.1}\text{O}_3$ , the situation is analogous to that discussed above for  $\text{La}_{1-\delta}\text{MnO}_3$  except that the NMR enhancement was found to be only slightly larger for FMM compared to FMI clusters. This fact leads to a more pronounced contribution of the fast relaxing com-

ponent to the spin-echo decay curves (Fig. 6), though the relative volume of the FMM clusters in the Ti-substituted sample, estimated from the  $^{55}\text{Mn}$  NMR, is about 10% of the total volume, while for  $\text{La}_{1-\delta}\text{MnO}_3$  it is only 1.5-3%. For both compounds the FMM volume practically do not change with the temperature. The relaxation for the FMI signal is very strongly temperature dependent and evidently there exists a distribution of the relaxation rates. As a consequence when relaxation rate increases, increasing part of the nuclear spins relaxes before it could be detected. This is the reason for gradual decrease and final disappearance of the FMI NMR signal, though they were corrected (Fig. 5). The number of Mn spins in the FMI clusters is in fact preserved as the magnetic moment in the corresponding temperature interval changes only slightly (Fig. 1b).

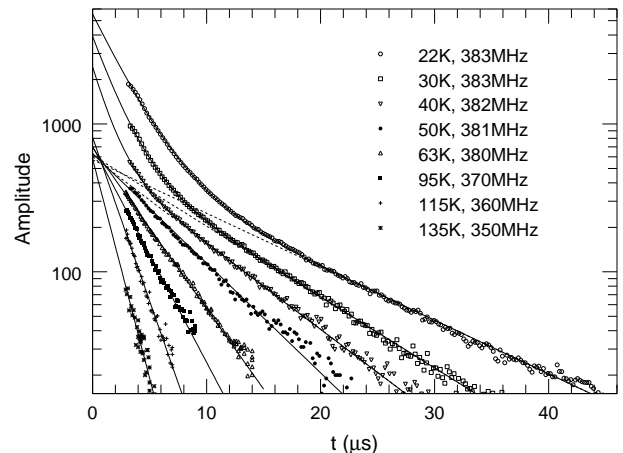


FIG. 6.  $\text{La}_{0.6}\text{Pb}_{0.4}\text{Mn}_{0.9}\text{Ti}_{0.1}\text{O}_3$ . Spin-echo decay taken at the maximum of the FMM line.

A metal-insulator transition occurs in  $\text{La}_{0.94}\text{Mn}_{0.98}\text{O}_3$  compound ( $T_{MI}=115$  K) and in  $\text{La}_{0.84}\text{Sr}_{0.16}\text{MnO}_3$  ( $T_{MI}=157$  K) and this is reflected in the corresponding NMR spectra. For  $\text{La}_{0.94}\text{Mn}_{0.98}\text{O}_3$  (Fig. 7) the amplitude of the FMM signal decreases considerably below  $\sim 150$  K pointing to the reduction of the summary volume of the FMM clusters around the MI transition (see also Fig. 10b). Below  $\sim 60$  K the FMI clusters are detected by NMR, their behavior being similar to the one described above. A quite different situation is found in the  $\text{La}_{0.84}\text{Sr}_{0.16}\text{MnO}_3$  compound. Here the FMM regions give the dominating contribution to the NMR spectrum in the whole temperature interval studied. However, below the MI transition the FMM NMR spectrum no longer consists of a single gaussian line as an obvious tail starts to develop on the low frequency side of the line. As discussed in detail elsewhere [20] this corresponds to a charge and/or orbital ordering in the FMM regions. Analogously to other three compounds a FMI signal can only be detected below  $\sim 60$  K, but because of the dominance of FMM signal, only the  $\text{Mn}^{4+}$  resonance can be distinguished unambiguously.

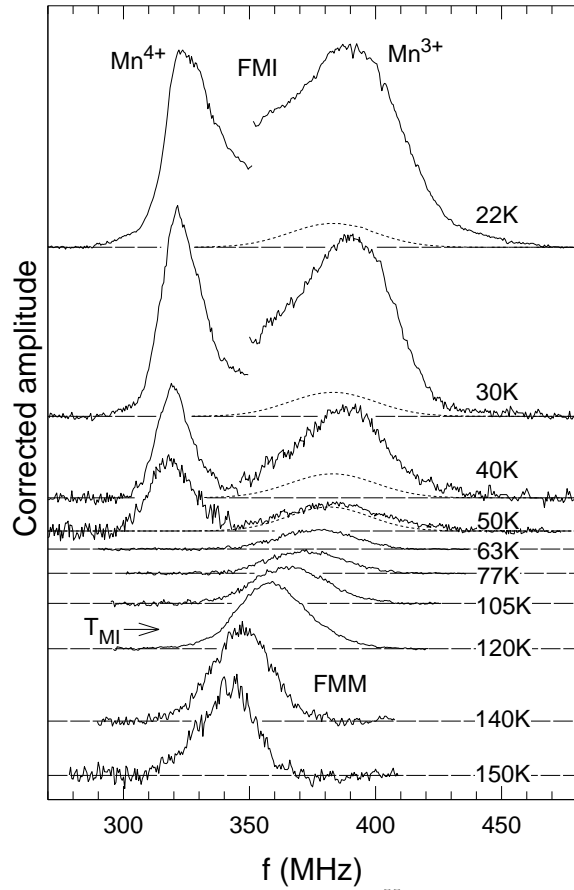


FIG. 7.  $\text{La}_{0.94}\text{Mn}_{0.98}\text{O}_3$ . Corrected  $^{55}\text{Mn}$  NMR spectra at several temperatures. The dotted curves correspond to the contribution of the FMM clusters to the spectra.

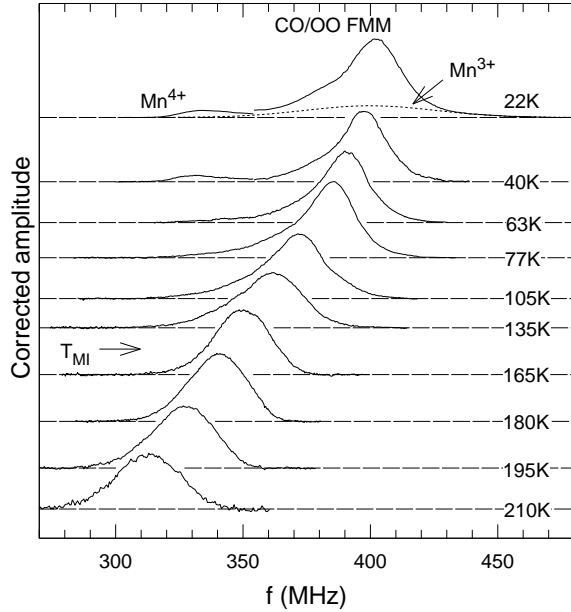


FIG. 8.  $\text{La}_{0.84}\text{Sr}_{0.16}\text{MnO}_3$ . Corrected  $^{55}\text{Mn}$  NMR spectra taken at several temperatures. The dotted line at the 22 K shows schematically the contribution of the  $\text{Mn}^{3+}$  ions.

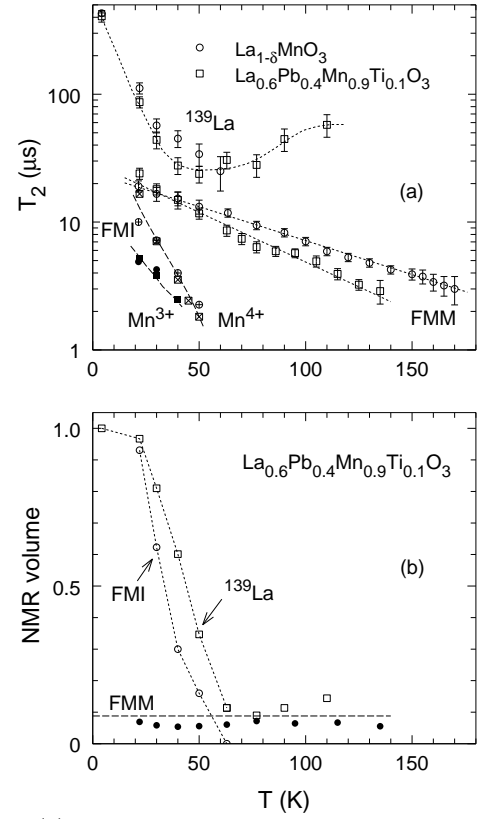


FIG. 9. (a) Temperature dependence of the spin-spin relaxation time  $T_2$  for  $^{55}\text{Mn}$  nuclei in the FMM and FMI clusters and for  $^{139}\text{La}$  nuclei. (b) Temperature dependence of the relative reduced volume of the FMM (●) and FMI (○) clusters determined from the areas under corresponding  $^{55}\text{Mn}$  NMR signals. □ denote the reduced volume determined from the area under the  $^{139}\text{La}$  signal.

The results of the analysis of the  $\text{La}_{1-\delta}\text{MnO}_3$  and  $\text{La}_{0.6}\text{Pb}_{0.4}\text{Mn}_{0.9}\text{Ti}_{0.1}\text{O}_3$  NMR spectra are displayed in Fig. 9. To obtain more complete information the  $^{139}\text{La}$  NMR was also studied for these compounds. The spin-spin relaxation on the La nuclei is strongly temperature dependent and it also becomes strongly inhomogeneous when the temperature increases, similarly as reported in [7,8]. Shown in Fig. 9a are the values of  $T_2(T)$  for  $^{55}\text{Mn}$  in FMI and FMM clusters as well as for the  $^{139}\text{La}$  where, as shown below, the contribution from the FMI clusters dominates at low temperatures, while at higher temperatures only the contribution from the FMM clusters remains. For  $\text{Mn}^{4+}$  and La, where the relaxation is non-exponential, the values of  $T_2$  determined from the tail ends of the spin-echo decay are presented. As seen from Fig. 3b this provides an appropriate characteristic of the evolution of the spin-echo decay with the temperature.

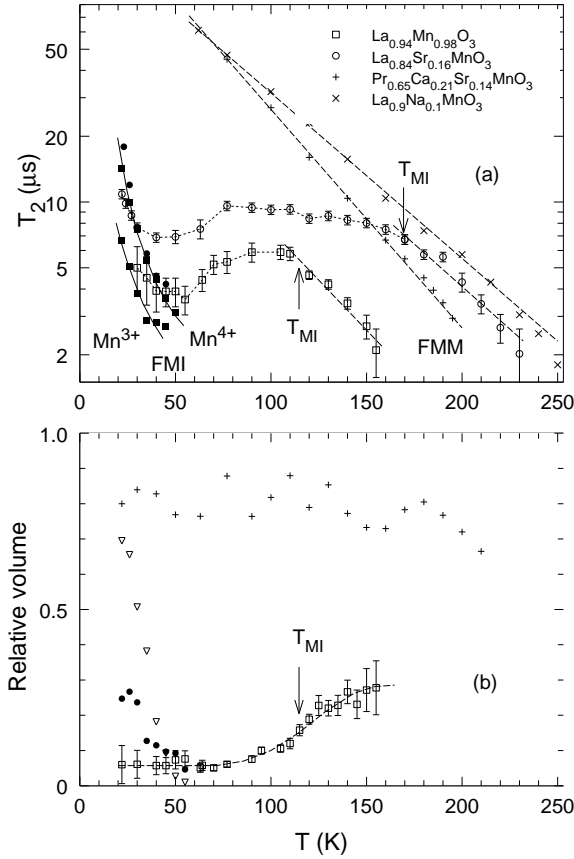


FIG. 10. (a) Temperature dependence of the spin-spin relaxation time  $T_2$  for  $^{55}\text{Mn}$  nuclei in the FMM and FMI clusters. For comparison the data for two metallic-like manganites  $\text{La}_{0.9}\text{Mn}_{0.1}\text{MnO}_3$  ( $T_C=266$  K) and  $\text{Pr}_{0.65}\text{Ca}_{0.21}\text{Sr}_{0.14}\text{MnO}_3$  ( $T_C=205$  K) are also displayed. (b) Temperature dependence of the relative volumes of the FMM and FMI clusters. For  $\text{La}_{0.94}\text{Mn}_{0.98}\text{O}_3$  the volumes of the FMM clusters are denoted by  $\square$ , the volume of the FMI clusters determined from the  $\text{Mn}^{4+}$  and  $\text{Mn}^{3+}$  line are denoted by  $\bullet$  and  $\nabla$ , respectively. For  $\text{La}_{0.84}\text{Sr}_{0.16}\text{MnO}_3$  only the FMM volume is displayed (+).

The form of temperature dependence of  $T_2$  in the FMM clusters is similar to the one found in the metallic-like manganites [18], though the relaxation is considerably faster. The  $^{55}\text{Mn}$  relaxation in the FMI clusters increases rapidly with the temperature, its behavior below 60 K being remarkably similar to that of  $^{139}\text{La}$ . This fact strongly suggests that in the FMI clusters the origin of the relaxation is the same for both nuclei. In the metallic-like manganites the  $^{55}\text{Mn}$  relaxation is due to the fluctuation of the hyperfine field induced by the hopping of the electron holes. This mechanism is, however, ineffective for the La nuclei and, as a consequence, the temperature dependence of  $T_2$  for La is flat and quite different from that of the Mn nuclei in this case [18]. The interconnection of the  $^{55}\text{Mn}$  and  $^{139}\text{La}$  relaxation in the FMI regions may be then understood as follows - the hopping of the holes is much slower comparing to the metallic manganites and the charge carriers may be represented as the JT small polarons, their movement being

accompanied by a lattice excitation leading to a fluctuation of the electric field gradient (EFG) on the La sites. Thus both the fluctuation of the EFG on the La sites and the fluctuation of the EFG and the hyperfine field on the Mn sites have the same characteristic time  $\tau_{JT}$  connected with the movement of the JT polaron which leads to similar temperature dependence of corresponding relaxations. Note that for the  $^{139}\text{La}$  relaxation this mechanism was recently proposed by Allodi *et al.* [7]. These authors showed that at temperatures below 60 K the  $^{139}\text{La}$  NMR in FMI manganites corresponds to the 'slow fluctuation' limit i.e.  $\tau_{JT} \gamma_n B_{hf} > 1$ . Therefore, the two lines we observe in the  $^{55}\text{Mn}$  NMR spectra of the FMI clusters correspond to 3+ and 4+ valence states of the Mn ion, which is the same conclusion as reached in [12]. Note that this situation corresponds to a slow hopping, rather than to a localization of the charge carriers as for the localized  $\text{Mn}^{3+}$  ions the NMR spectrum is strongly anisotropic and the nuclear spin-lattice relaxation time  $T_1$  is very short. In this situation the spin-spin relaxation is governed by the spin-lattice channel with a limiting relation  $T_2=2T_1$ . In contrast, down to 22 K the spin-lattice relaxation for both  $\text{Mn}^{4+}$  and  $\text{Mn}^{3+}$  lines was checked to be relatively slow with a ratio  $T_1/T_2 \approx 30-60$  in all compounds in question. Rather surprising proximity of  $f_{\text{res}}$   $\text{Mn}^{3+}$  in the FMI clusters and  $f_{\text{res}}$  of the motionally narrowed line in the FMM clusters could be connected with different local distortions in these two types of clusters.

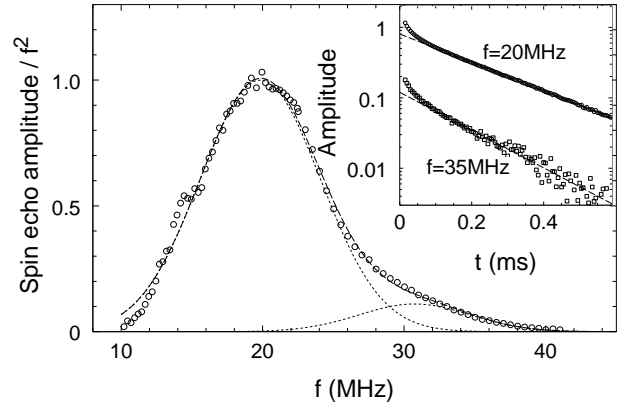


FIG. 11.  $\text{La}_{1-\delta}\text{MnO}_3$ .  $^{139}\text{La}$  NMR spectrum at 4.2 K and its decomposition. In the inset the spin-echo decay at two frequencies around the maxima of the two components of the spectrum are shown.

The temperature dependence of the normalized amplitudes of the  $^{55}\text{Mn}$  signal from FMI (summing the  $\text{Mn}^{3+}$  and  $\text{Mn}^{4+}$  contributions) and FMM clusters are compared with the normalized amplitude of the  $^{139}\text{La}$  signal which was corrected for observed  $T_2$  in Fig. 9b. It is clearly seen that above 60 K the La signal comes from the FMM clusters, while at lower temperatures its increase is connected with the contribution from the FMI regions. Note that the recovery of the signal from the

FMI regions has a similar character for both Mn and La nuclei.

The results of the analysis of  $^{55}\text{Mn}$  NMR spectra in  $\text{La}_{0.94}\text{Mn}_{0.98}\text{O}_3$  and  $\text{La}_{0.84}\text{Sr}_{0.16}\text{MnO}_3$  are displayed in Fig. 10. The NMR relaxation in the FMI clusters is analogous to that described above, while its behavior in the FMM clusters is more complex and intriguing. Above the metal-insulator transition the temperature dependence of the relaxation is exponential-like as in metallic manganites though for  $\text{La}_{0.94}\text{Mn}_{0.98}\text{O}_3$  the magnitude of  $T_2$  is considerably smaller, below  $T_{MI}$  it becomes more flat for both compounds exhibiting a minimum at  $\sim 50$  K (Fig. 10a). This can be naturally connected to the slow fluctuations which in the same temperature region lead to the disappearance of the NMR signal in the FMI clusters. Such attribution of the minima in  $T_2$  implies that there is a hyperfine coupling between the JT small polarons existing in the FMI clusters and  $^{55}\text{Mn}$  nuclear spins in the FMM clusters, i.e. the FMI and FMM systems are closely intertwined. It is interesting to note in this context that for  $\text{La}_{0.94}\text{Mn}_{0.98}\text{O}_3$  the decrease of the volume of FMM clusters (Fig. 10b) is accompanied by a reduction of the NMR enhancement factor approx. 1.7 times between 120 and 77 K, and at lower temperatures it becomes close to the NMR enhancement for FMI clusters. On the other hand, for  $\text{La}_{1-\delta}\text{MnO}_3$  and  $\text{La}_{0.6}\text{Pb}_{0.4}\text{Mn}_{0.9}\text{Ti}_{0.1}\text{O}_3$  samples no visible minima in  $T_2$  for FMM signal is observed (Fig. 9a). This may imply that for these systems the minority FMM regions and the FMI matrix are less intimately intertwined.

As mentioned above, a satellite of the  $\text{Mn}^{4+}$  line in the  $^{55}\text{Mn}$  spectrum at  $\sim 300$  MHz is observed in  $\text{La}_{1-\delta}\text{MnO}_3$  (Fig. 2). The splitting  $\sim 25$  MHz is too large to be explained by the change of the dipolar or/and supertransferred fields it could be, however, caused by a redistribution of the spin density around specific Mn sites. Such redistribution, decreasing local spin density on the Mn site would lead to an increase of the transferred hyperfine interaction on the nearest La sites due to the enhanced Mn-O covalency. Indeed an unresolved satellite line on the high frequency side of the  $^{139}\text{La}$  spectrum is detected in this compound as seen in Fig. 11. Interestingly a similar high frequency tail of the La NMR was observed in the (LaCa) manganites [8,21], while a satellite in the  $^{55}\text{Mn}$  spectra could be found in the results reported for these compounds and for a self-doped  $\text{LaMnO}_3$  [10].

Let us present now a general picture of FMI state in manganites which can be inferred from the above described results. Perturbations in these systems hinder the motion of the charge carriers, reducing thus the strength of the DE interaction. Slower hopping of the electron holes increases the role of their interaction with the lattice and, as a result, the clusters where charge carriers can be viewed as JT small polarons grow at the expense of the metallic-like host. The resulting state may be ferromagnetic insulating if the polaronic regions dominate ( $\text{La}_{1-\delta}\text{MnO}_3$ ,  $\text{La}_{0.6}\text{Pb}_{0.4}\text{Mn}_{0.9}\text{Ti}_{0.1}\text{O}_3$ ), or the transition to metallic like conductivity with relatively high resistiv-

ity may occur through the percolation of the FMM clusters as their total volume increases with increasing temperature ( $\text{La}_{0.94}\text{Mn}_{0.98}\text{O}_3$ ). A specific case represents the system  $\text{La}_{0.84}\text{Sr}_{0.16}\text{MnO}_3$ , where the insulator to metal transition in the FM state is due to the breakdown of charge and/or orbital ordering in the FMM regions. Accordingly, the resistivity in ferromagnetic metallic state is closer to the one in conventional manganites in this case. The minority polaronic regions are also detected for  $\text{La}_{0.84}\text{Sr}_{0.16}\text{MnO}_3$  and we expect that their role will increase for the lower doping. This may explain the different behavior of FMI state in  $\text{La}_{1-x}\text{Sr}_x\text{MnO}_3$  for slightly different  $x$ , in particular for  $0.1 \leq x \leq 0.14$  the FMI state is stabilized under pressure and field [4,6], while for  $x=0.15$ , 0.16 the FMI state is suppressed by pressure [6,22]. Further NMR experiments are required to clarify the problem.

The effect of the inhomogeneity on the motion of the charge carriers, that is the distribution of the activation energies of JT polaron hopping seems to be similar for all cases, leading to disappearance of the signals on Mn nuclei at  $T \sim 60$  K. An analogous behavior was found in  $\text{La}_{0.825}\text{Ca}_{0.175}\text{MnO}_3$  [11]. Also  $\text{Mn}^{4+}$  resonance in  $\text{La}_{0.9}\text{Ca}_{0.1}\text{MnO}_3$  was detected up to 77 K only [10]. Further, the disappearance or reduction of the amplitude of signal on the La nuclei was reported for a number of self-doped and (LaCa) manganites at the temperature range 50-100 K in Refs. [7,8] and it is the same behavior as detected for  $\text{La}_{1-\delta}\text{MnO}_3$  and  $\text{La}_{0.6}\text{Pb}_{0.4}\text{Mn}_{0.9}\text{Ti}_{0.1}\text{O}_3$  samples in the present study. All these facts suggest that the polaronic state is an intrinsic response of the DE system to the perturbation rather than being specific for a given type of disorder. Thus at least for the FMI system with  $T_C \sim 150$ -200 K the ferromagnetic state is still controlled by DE through thermally activated hopping of small JT polarons. On the other hand even for strongly disordered  $\text{La}_{1-\delta}\text{MnO}_3$  a small fraction of the fast hopping holes survives in the polaronic host. This rises the question whether the JT polarons can alone produce the long range ferromagnetic ordering, or a small fraction of the fast hopping holes is an essential component of the FMI state.

The NMR signals arising from the FMI clusters correspond to the slow fluctuation limit which means the freezing of the polarons on a time scale comparable to the duration of a NMR spin-echo experiment. Different mechanisms including quasistatistical orbital [8] and charge ordering [7] have been suggested in the literature in order to explain the corresponding ground magnetic state. The quasistatistical orbital hypothesis is based on observation of a high frequency tail in  $^{139}\text{La}$  NMR spectra of (LaCa) manganites at low temperatures. We also found such a feature in the  $\text{La}_{1-\delta}\text{MnO}_3$  but it is absent in the  $\text{La}_{0.6}\text{Pb}_{0.4}\text{Mn}_{0.9}\text{Ti}_{0.1}\text{O}_3$  spectra. Also the corresponding satellite line in  $^{55}\text{Mn}$  spectra is detected only for  $\text{La}_{1-\delta}\text{MnO}_3$ . We conclude therefore that this can hardly serve as a characteristic feature of the FMI state. Moreover even a short range orbital ordering seems to be un-

likely in the case of the strongly disordered  $\text{La}_{1-\delta}\text{MnO}_3$ . An alternative possibility may be a cluster-glass state. Such a state has been detected by specific heat and magnetic measurements in self-doped manganites  $\text{LaMnO}_{3+\delta}$  [5]. In particular, authors of Ref. [5] observed low temperature peak of the imaginary component of susceptibility, the position of which strongly depends on the measuring frequency. Shown in Fig. 12 is the ac susceptibility of  $\text{La}_{1-\delta}\text{MnO}_3$  sample. The frequency dependence of the real and imaginary part of the susceptibility as well as their absolute values are indicative of the cluster glass behaviour similarly as reported by Ghivelder *et al.* The situation may be similar to that observed in the lanthanum cuprates, where slowing down of the spin and/or charge fluctuations results in a strong peak in the spin-lattice relaxation for the La nuclei and in a loss of signal on the Cu nuclei and it is ascribed to the glassy magnetic state [23–25]. It is interesting that for both Cu and La signals stretched exponential like spin-echo decay is observed in the slow fluctuation limit similarly to the one for FMI signals in manganites, while in the motionally narrowed limit, below a transition temperature  $T_{\text{charge}}$ , corresponding to the localization of charge-ordered stripes, a Lorentzian single-exponential spin-echo decay is detected [24,26,27].

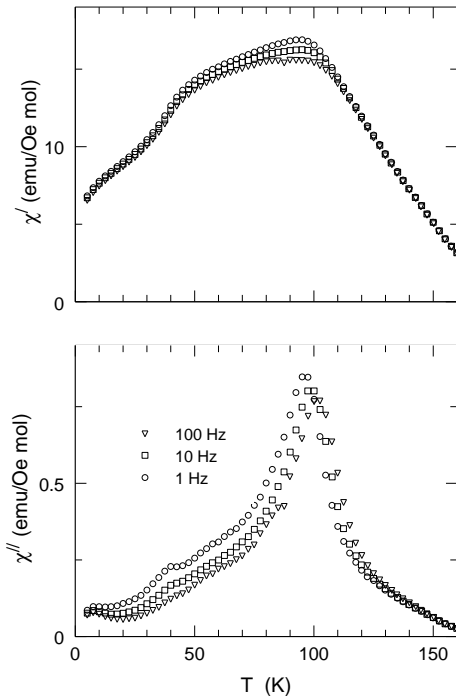


FIG. 12. Temperature dependence of the ac susceptibility for 1, 10 and 100 Hz for  $\text{La}_{1-\delta}\text{MnO}_3$ .

#### IV. CONCLUSIONS

The study of  $^{55}\text{Mn}$  NMR in four manganites, in which the ferromagnetic insulating state is caused by diverse reasons, showed that in all cases the metallic-like (FMM,

$f_{\text{hop}} > \Delta f_{\text{res}}$ ) and insulating (FMI,  $f_{\text{hop}} < \Delta f_{\text{res}}$ ) regions coexist, though the ratio of their volumes differs considerably in different compounds. The dynamics of the nuclear spins in the FMI clusters is almost independent of the compound, pointing to similarity of the charge carrier dynamics, despite the different origin of the FMI state in the manganites studied. The temperature dependence of  $^{139}\text{La}$  and  $^{55}\text{Mn}$  relaxation in the FMI clusters is analogous which can be understood as due to the EFG fluctuation on the La nuclei and combined EFG and hyperfine field fluctuation on Mn nuclei connected with the motion of the Jahn-Teller polaron. In two compounds with the metal-insulator transition the temperature dependence of the relaxation rate in FMM and FMI clusters indicates that these two types of regions should be intertwined on a microscopic scale. In the self-doped  $\text{La}_{0.94}\text{Mn}_{0.98}\text{O}_3$  the insulator to metal transition occurs because of the percolation of the FMM clusters, as their total volume increases with increasing temperature, while in  $\text{La}_{0.84}\text{Sr}_{0.16}\text{MnO}_3$  the reason is the breakdown of the charge and/or orbital ordering. Finally we suggest that the FMI state in manganites may be viewed as a cluster-glass, which is supported by the character of the temperature and frequency dependence of the ac susceptibility.

We are grateful to Y. Tomioka and to M. Greenblatt for providing  $\text{La}_{0.84}\text{Sr}_{0.16}\text{MnO}_3$  and  $\text{La}_{0.94}\text{Mn}_{0.98}\text{O}_3$  single crystals, respectively. We also thank to T. N. Tarasenko for sintering the  $\text{La}_{1-\delta}\text{MnO}_3$  polycrystal, to V. D. Doroshev for measuring the resistivity of  $\text{La}_{1-\delta}\text{MnO}_3$ , to J. Englich and J. Kohout for providing the possibility of  $^{139}\text{La}$  NMR measurements at liquid helium temperature at the coherent spectrometer at the Charles University, Prague. This work was supported by the grant 202/00/1601 of Grant Agency of the Czech Republic and grant A1010202 of the Grant Agency of AS CR.

- 
- [1] E. Dagotto, T. Hotta, and A. Moreo, *Physics Reports* **344**, 1 (2001).
  - [2] Y. Yamada, O. Hino, S. Nohdo, R. Kanao, T. Inami, and S. Katano, *Phys. Rev. Lett.*, **77**, 904 (1996).
  - [3] Y. Endoh, K. Hirota, S. Ishihara, S. Okamoto, Y. Murakami, A. Nishizawa, T. Fukuda, H. Kimura, H. Nojiri, K. Kaneko, and S. Maekawa, *Phys. Rev. Lett.*, **82**, 4328 (1999).
  - [4] B. Martinez, R. Senis, L. Balcells, V. Laukhin, J. Fontcuberta, L. Pinsard, and A. Revcolevschi, *Phys. Rev. B* **61**, 8643 (2000).
  - [5] L. Ghivelder, I.A. Castillo, M. A. Gusmão, J.A. Alonso, and L.F. Cohen, *Phys. Rev. B* **60**, 12 184 (1999).
  - [6] J.-S. Zhou, J. B. Goodenough, A. Asamitsu, and Y. Tokura, *Phys. Rev. Lett.* **79**, 3234 (1997).
  - [7] G. Allodi, M. C. Guidi, R. De Renzi, A. Caneiro, and L. Pinsard, *Phys. Rev. Lett.* **87**, 127206 (2001).



- [8] G. Papavassiliou, M. Belesi, M. Fardis, and C. Dimitropoulos, Phys. Rev. Lett. **87**, 177204 (2001).
- [9] Cz. Kapusta and P. C. Riedi, J. Magn. Magn. Mater. **196-197**, 446 (1999).
- [10] Cz. Kapusta, P. C. Riedi, W. Kocemba, M. R. Ibarra, and J. M. D. Coey, J. Appl. Phys. **87**, 7121 (2000).
- [11] M. Belesi, G. Papavassiliou, M. Fardis, J. E. Wegrone, and C. Dimitropoulos, Phys. Rev. B **63**, 180406(R) (2001).
- [12] G. Allodi, M. C. Guidi, R. De Renzi, and M. W. Pieper, J. Magn. Magn. Mater. **242-245**, 635 (2002).
- [13] V. Markovich, E. Rozenberg, G. Gorodetsky, M. Greenblatt, and W. H. McCarroll, Phys. Rev. B **63**, 054423 (2001).
- [14] M. Sahana, K. Döerr, M. Doerr, D. Eckert, K.-H. Müller, K. Nenkov, L. Schults, and M. S. Hegde, J. Magn. Magn. Mater. **213**, 253 (2000).
- [15] X. Liu, X. Xu, and Y. Zhang, Phys. Rev. B **62**, 15 112 (2000).
- [16] D. Cao, F. Bridges, M. Anderson, A. P. Ramirez, M. Olapinski, M. A. Subramanian, C. H. Booth, and G. H. Kwei, Phys. Rev. B **64**, 184409 (2001).
- [17] G. Matsumoto, J. Phys. Soc. Jpn. **29**, 615 (1970).
- [18] M. M. Savosta, V. A. Borodin, and P. Novák., Phys. Rev. B **59**, 8778 (1999).
- [19] M. M. Savosta and P. Novák., J. Magn. Magn. Mat. **242-245**, 672 (2002).
- [20] M. M. Savosta, P. Novák, and Z. Jiráček, submitted to Phys. Rev. Lett.
- [21] Y. Yoshinari, P. C. Hammel, J. D. Thompson, and S.-W. Cheong, Phys. Rev. B **60**, 9275 (1999).
- [22] Y. Moritomo, A. Asamitsu, and Y. Tokura, Phys. Rev. B **56**, 12 190 (1997).
- [23] M.-H. Julien, F. Borsa, P. Carretta, M. Horvatić, C. Berthier, and C. T. Lin, Phys. Rev. Lett. **83**, 604 (1999).
- [24] A. W. Hunt, P. M. Singer, A. F. Cederström, and T. Imai, Phys. Rev. B **64**, 134525 (2001).
- [25] N. J. Curro, P. C. Hammel, B. J. Suh, M. Hücker, B. Büchner, U. Ammerahl, and A. Revcolevschi, Phys. Rev. Lett. **85**, 642 (2000).
- [26] G. B. Teitelbaum, B. Büchner, and H. de Gronckel, Phys. Rev. Lett. **84**, 2949 (2000).
- [27] A. W. Hunt, P. M. Singer, K. R. Thurber, and T. Imai, Phys. Rev. Lett. **82**, 4300 (1999).